Biology of Reproduction, 2020, 103(5), 966–977
doi:10.1093/biolre/ioaa146
Research Article
Advance Access Publication Date: 21 August 2020

OXFORD

Research Article

Aberrant and constitutive expression of FOXL2 impairs ovarian development and functions in mice

Barbara Nicol*, Karina Rodriguez and Humphrey H.-C. Yao*

Reproductive and Developmental Biology Laboratory, National Institute of Environmental Health Sciences, Research Triangle Park, NC 27709, USA

***Correspondence:** Barbara Nicol and Humphrey H-C Yao, Reproductive and Developmental Biology Laboratory, National Institute of Environmental Health Sciences (NIEHS/NIH), 111 T.W. Alexander Dr, Mail Drop C4-10, Research Triangle Park, NC 27709 USA. Emails: barbara.nicol@nih.gov and humphrey.yao@nih.gov

Grant support: This research was supported by the Intramural Research Program (Z01ES102965 to HHCY) of the NIH, National Institute of Environmental Health Sciences.

Received 24 April 2020; Revised 7 August 2020; Accepted 18 August 2020

Abstract

Development and functions of the ovary rely on appropriate signaling and communication between various ovarian cell types. FOXL2, a transcription factor that plays a key role at different stages of ovarian development, is associated with primary ovarian insufficiency and ovarian cancer as a result of its loss-of-function or mutations. In this study, we investigated the impact of aberrant, constitutive expression of FOXL2 in somatic cells of the ovary. Overexpression of FOXL2 that started during fetal life resulted in defects in nest breakdown and consequent formation of polyovular follicles. Granulosa cell differentiation was impaired and recruitment and differentiation of steroidogenic theca cells was compromised. As a consequence, adult ovaries overexpressing FOXL2 exhibited defects in compartmentalization of granulosa and theca cells, significant decreased steroidogenesis and lack of ovulation. These findings demonstrate that fine-tuned expression of FOXL2 is required for proper folliculogenesis and fertility.

Summary Sentence

Constitutive expression of FOXL2 results in defects in granulosa cell and theca cell differentiation, ultimately impairing folliculogenesis, steroidogenesis and ovulation.

Key words: FOXL2, ovary, folliculogenesis, granulosa, theca, fertility.

Introduction

The two main functions of the ovary are to produce female gametes (oocytes) and to secrete hormones that facilitate communications among reproductive organs. These two functions are the product of a highly orchestrated process called folliculogenesis, which involves cross-talks among key cell populations: oocytes, granulosa cells, the surrounding theca cells, and the ovarian interstitium. Misregulation of cross-talk among these cell types can lead to either improper follicle formation or impaired follicular function, the underlying causes of primary ovarian insufficiency (POI)/infertility, ovarian disorders such as polycystic ovarian syndrome (PCOS), and even cancer. Among the cell types composing the ovary, granulosa cells play a unique role in supporting the development of oocytes within the follicles and the recruitment and differentiation of theca cells for proper steroidogenesis [1–4]. Disruption of granulosa cell differentiation or mis-expression of granulosa cell genes are known to

associate with ovarian defects and pathologies. For instance, mutations in the gene forkhead box L2 (*FOXL2*), encoding a key transcription factor in granulosa cells, are responsible for the autosomal dominant Blepharophimosis Ptosis Epicanthus inversus Syndrome (BPES) in humans [5]. A characteristic of type 1 BPES includes primary ovarian insufficiency, which is defined as a loss of normal ovarian function before the age of 40 years. Comparisons of various *FOXL2* mutations responsible for BPES suggest that primary ovarian insufficiency is correlated with a loss of transcriptional activity of FOXL2 [6]. In addition to BPES, mutations in *FOXL2* have also been associated with non-syndromic primary ovarian insufficiency [7, 8]. FOXL2 is also involved in ovarian malignancy as a result of a specific missense mutation (c.402C > G, p.C134W), which is found in the majority of adult granulosa cell tumors [9]. This missense mutation alters FOXL2 capacity to regulate cell-cycle [10], apoptosis [11] and steroidogenesis [12] in the ovary. *FOXL2* is a single exon gene whose sequence is highly conserved in vertebrates [13]. In the ovary, FOXL2 is one of the first markers for granulosa cells [14–16]. *Foxl2* global knockout in the mouse results in a phenotype that recapitulates some aspects of type 1 BPES syndrome in humans, with a blockage of follicle formation postnatally, followed by follicle degeneration, ultimately causing infertility [16, 17]. In multiple species, FOXL2 promotes ovarian differentiation and antagonizes the appearance of molecular programs for testis differentiation [18–20]. *Foxl2* knockout ovaries express testis-specific genes postnatally [21], and conditional loss of *Foxl2* in mouse adult ovaries leads to transdifferentiation of granulosa cells into testicular Sertoli-like cells [22], suggesting a key role of FOXL2 in maintenance of granulosa cell identity. In the fetal ovary, FOXL2 acts synergistically with the RSPO1/WNT pathway [23, 24] and RUNX1 [25] to induce/maintain fetal granulosa cell identity. Overall, animal models and human clinical cases demonstrate that FOXL2 is important at multiple stages of ovarian physiology, from early cell differentiation to folliculogenesis. In this study, we investigated the consequences of FOXL2 mis-expression on folliculogenesis, steroidogenesis, cell differentiation, and reproductive functions of the ovary by developing a mouse model that constitutively expresses FOXL2 in the somatic cells of the ovary.

Materials and methods

Mouse model for induction of constitutive FOXL2 expression

Generation of the *Rosa-Foxl2* mice was previously described [26]. In brief, we designed the *Rosa26-CAG-LSL-Foxl2* construct that allows conditional expression of *Foxl2* only in the presence of Cre recombinase that removes the stop cassette 5′ of the *Foxl2* cassette. In addition, the construct contains a 6xHis-tag (His) that permits detection of the ectopic FOXL2 protein. To target *Foxl2* induction in somatic cells of ovaries, *Rosa-Foxl2* mice were crossed to *Sf1-Cre* mice (Tg (Nr5a1-cre)2Klp) [27], which have been used extensively by us and others [28–30] (Figure 1A). The genetic background of these mice was mixed C57BL/6 J and 129Sv. The Cre recombinase expression under the control of *Nr5a1* regulatory elements allowed the conditional induction of FOXL2-His in the somatic cells of undifferentiated gonads around embryonic day E11 [26]. For timed mating, noon on the day when the vaginal plug was observed was considered E0.5. The genotypes of females overexpressing FOXL2 (named FOXL2+ thereafter) and their control female littermates were *Rosa-Foxl2*$^{+/f}$; *Sf1-Cre*$^{Tg/+}$ and *Rosa-Foxl2*$^{+/+}$; *Sf1-Cre*$^{Tg/+}$, respectively (Figure 1A). All animal procedures were approved by the National Institute of Environmental Health Sciences (NIEHS) Animal Care and Use Committee and were in compliance with a NIEHS-approved animal study proposal.

Immunofluorescence, TUNEL assay and histological analyses

Ovaries were collected and fixed overnight at 4 °C in 4% paraformaldehyde. Immunofluorescence experiments were performed on 5 µm paraffin sections or 8 µm cryosections. For paraffin-embedded tissues, sections were dewaxed and rehydrated in a decreasing gradient of alcohol. The slides were pretreated in 0.1 mM citric acid (Vector Labs) for 20 min in the microwave, and cooled down to room temperature. All samples (paraffin and cryosections) were blocked in PBS-Triton X-100 solution with 5% normal donkey serum for 1 hour, and incubated with primary antibodies at 4 °C overnight. After washing in PBS-Triton X-100, samples were incubated with the secondary antibody (1: 300; Invitrogen), then washed again, counterstained with DAPI, and mounted in ProLong™ Diamond Antifade Mountant (ThermoFisher). The following primary antibodies were used: FOXL2 (1: 300; Novus NB100–1277), Steroidogenic Factor-1 NR5A1 (1: 500; a kind gift from Ken-ichirou Morohashi), HIS-Tag (1: 300; Abcam ab9108), DDX4 (1: 500; Abcam ab13840), LAMININ (1: 300; Sigma L9393), TRA98/GNCA (1, 500; Abcam ab82527), HSD3B (1, 500; CosmoBio K0607), aSMA (1, 500; Abcam ab5694), CYP17A1 (1, 200; Santa Cruz sc-46081), NR2F2 (1, 300; R&D Systems PP-H7147–10), AMH (1, 500; Santa Cruz sc-6886) and WT1 (1, 300; Abcam ab15249). The following secondary antibodies were used at 1: 300 dilution (Invitrogen/Life Technology): Donkey anti-goat Alexa 647 (A21447), Donkey anti-mouse Alexa 568 (A10037), Donkey anti-rat Alexa 594 (A21209), Donkey anti-rabbit Alexa 488 (A21206), and Donkey anti-rabbit Alexa 568 (A10042).

Cell death was determined using the In-Situ Cell Death Detection Kit Fluorescein (Roche) following the manufacturer's instruction. Briefly, the paraffin slides were subjected to an immunofluorescence protocol for Laminin and FOXL2 as described above. After the secondary antibody washes, the slides were incubated in the TUNEL labeling solution for 1 h at 37 °C, washed in PBS, counterstained in DAPI and mounted. Sections for immunofluorescence and TUNEL assay were imaged under a Leica DMI4000 confocal microscope.

Histological analysis was performed by staining dewaxed paraffin sections with hematoxylin and eosin. The stained sections were scanned using Aperio ScanScope XT Scanner (Aperio Technologies, Inc., CA, USA).

Polyovular follicle incidence

Ovaries at postnatal day 9 were serially sectioned at 5 µm thickness and immunofluorescence was performed for DDX4 and FOXL2. Follicles were counted on 8 representative sections at 50 µm interval for 4 ovaries per genotype. Polyovular follicles were defined as follicles containing more than one oocyte. The incidence of polyovular follicles for each ovary was calculated as the mean percentage value of polyovular follicles over total follicles per section.

RNA extraction and Real-Time PCR analysis

Ovaries were separated from the mesonephros/reproductive tract before being snap-frozen for RNA extraction. For E14.5 ovaries, six biological replicates were used per genotype. For postnatal day 9 (P9) ovaries, seven and eight biological replicates were used for control

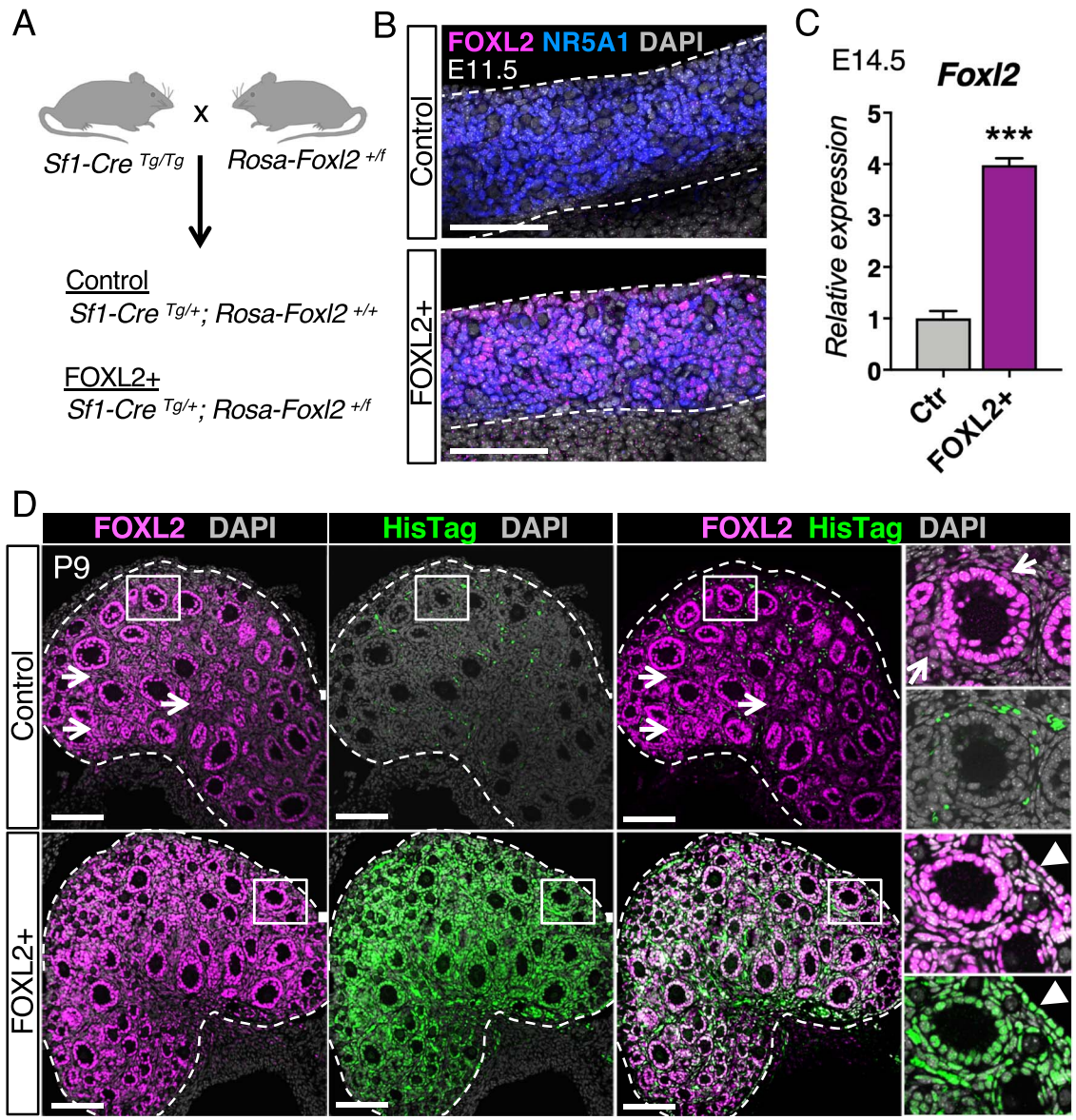

Figure 1. Constitutive induction of FOXL2 in somatic cells of the ovary. (A) Mouse model for constitutive induction of FOXL2 in the ovarian somatic cells. The Rosa-Foxl2$^{+/f}$ mice were crossed with *Sf1*-Cre$^{Tg/Tg}$ mice to produce control and mutant FOXL2+ mice. (B) Immunofluorescence for FOXL2 (magenta), Steroidogenic Factor-1 NR5A1 (blue), and nuclear counterstain DAPI (grey) in control and FOXL2+ ovaries at E11.5. Dotted lines outline the ovaries. Scale bar: 100 µm, n = 4/genotype. (C) qPCR analysis of *Foxl2* expression in control and FOXL2+ ovaries at E14.5 The data were analyzed with Student t-test; Bar graphs represent mean ± SEM (n = 6/genotype); ***P < 0.001. (D) Immunofluorescence for total FOXL2 (magenta), ectopic FOXL2 with HisTag (green), and nuclear counterstain DAPI (grey) in control and FOXL2+ ovaries at postnatal day 9 (P9). Dotted lines outline the ovaries. Right panels represent higher magnification images of the outlined area for each single fluorescent channel. Arrows and arrowheads indicate FOXL2+ interstitial cells and FOXL2+ ovarian surface epithelium, respectively. The signal for HisTag in the control ovary came from the autofluorescence of blood cells. Scale bar: 100 µm; n = 4/genotype.

and FOXL2+ ovaries respectively. For both E14.5 and P9 ovaries, we used Arcturus PicoPure extraction kit (Thermo Fisher) for total RNA isolation. For adult ovaries, six and four biological replicates were used for control and FOXL2+ ovaries, respectively, and total RNA was isolated using RNeasy Mini kit (Qiagen). RNA quality and concentration were determined using the Nanodrop 2000c. cDNA synthesis was performed with total RNA (300 ng for E14.5 and P9 ovaries and 1 µg of RNA for 8-week-old ovaries) and the Superscript II cDNA synthesis system (Invitrogen Corp., Carlsbad, CA). Gene expression was analyzed by real-time PCR using Bio-Rad CFX96TM Real-Time PCR Detection system. Gene expression was normalized to *Gapdh*. The Taqman probes or primers used to detect transcript expression are listed in Supplementary Table S1.

Estrous cycle assessment

To assess the phases of the estrous cycle, vaginal smears were performed on 7-week old females by washing the vagina with 50 µL of sterile 0.9% NaCl daily for 3 weeks (n = 5 mice/genotype). Vaginal smears were mounted on slides and fixed with a cytology fixative spray (Safetex). The slides were stained with Harris Hematoxylin and observed under a light microscope. Each estrous cycle

stage (proestrus, estrus, metestrus and diestrus) was determined as previously described [31]. Data were analyzed using Prism 7 GraphPad Software and presented as the mean value of the percentage of days each stage was observed.

Hormone measurement

Serum samples of 6 FOXL2+ females and 6 control females in diestrus were collected at 8 weeks of age and stored at −80 °C until analyzed. Serum measurements were performed by the University of Virginia Center for Research in Reproduction Ligand Assay and Analysis Core. Serum levels of FSH and LH were determined in duplicates using the Pituitary Panel Multiplex kit (EMD Millipore), with a reportable range of 0.24–30.0 ng/mL for LH and 0.48–300.0 ng/mL for FSH, intra-assay CV of 5.1% and inter-assay CV of 9.6%. Progesterone was measured in duplicates by competitive enzyme immunoassay ELISA (IBL IB79183) with a reportable range of 0.150–40.00 ng/mL, intra-assay CV of 6.5% and inter-assay CV of 10.3%. Estradiol was measured in duplicates by competitive enzyme immunoassay ELISA (Calbiotech ES180S-100) with a reportable range of 3–300 pg/mL, intra-assay CV of 7.5% and inter-assay CV of 10.1%.

Statistical analyses

Data were analyzed with Prism 7 GraphPad Software. The normal distribution was determined using the Shapiro–Wilk test. Comparison between control and FOXL2+ groups for polyovular follicle incidence and transcript expression at E14.5 and P9 were evaluated using Student t-test. Serum hormone assays and transcript expression at 8 weeks old were analyzed using Mann–Whitney test. Values are presented as mean ± S.E.M. ns: non-significant; ∗: $p < 0.05$; ∗∗: $p < 0.01$; and ∗∗∗: $p < 0.001$.

Results

Characterization of constitutive induction of FOXL2 in somatic cells of the ovary

Under normal circumstances, FOXL2 first appears in the pre-granulosa cells of fetal ovaries, and its expression in granulosa cells progressively decreases as the follicles reach preantral stage [14, 17]. FOXL2 is also weakly expressed in some interstitial cells, including theca cells [2, 17, 32, 33] (Supplementary Figure S1). To determine the consequences of constitutive over-expression of FOXL2 in somatic cells of the ovaries, we crossed the *Rosa-Foxl2* mice [26] with *Sf1-Cre* mice [27] to produce control and FOXL2+ mutant females (Figure 1A). Whole mount immunofluorescence for FOXL2 and Steroidogenic Factor-1 NR5A1 demonstrated that in contrast to control ovaries where FOXL2 was not yet induced in granulosa cells at E11.5 [14], constitutive expression of FOXL2 was detected in most NR5A1+ somatic cells at E11.5 (Figure 1B). At E14.5, *Foxl2* mRNA expression in FOXL2+ ovaries was about 4 folds higher than that in the control ovaries (Figure 1C). At postnatal day 9, folliculogenesis had already initiated and ovaries contained primary and early secondary follicles (Figure 1D). In control ovaries, as expected, FOXL2 was strongly detected in nuclei of granulosa cells, and at lower levels in a subpopulation of cells in the interstitium (Figure 1D; arrows). In FOXL2+ ovaries, ectopic FOXL2 was specifically detected with an antibody against HisTag that was included in the targeting construct (Figure 1D, green) while the FOXL2 antibody detected both endogenous and ectopic FOXL2 proteins (Figure 1D, magenta). Ectopic FOXL2 was induced in granulosa cells, most of the interstitial cells, and the ovarian surface epithelium (Figure 1D, arrowheads).

Constitutive expression of FOXL2 in ovarian somatic cells leads to defects in nest breakdown and formation of polyovular follicles

At postnatal day 9, ovaries of control and FOXL2+ mice were grossly indistinguishable (Figure 2A). However, histological analyses revealed some defects in germ-cell nest breakdown in the FOXL2+ ovaries (Figure 2B and Supplementary Figure S2). Germ-cell nest breakdown is the phenomenon that progressively convert ovigerous cords, composed of syncytia of oocytes enclosed by granulosa cells, into primordial follicles, composed of a single oocyte surrounded by a layer of granulosa cells [for review, see 34]. In control ovaries, nest breakdown was nearly completed and almost all oocytes were separated from each other at postnatal day 9 (Supplementary Figure S2). Each DDX4-positive oocyte was fully surrounded by a layer of FOXL2-positive granulosa cells (Figure 2B). In contrast, in FOXL2+ ovaries, clusters of oocytes remained in nests (Supplementary Figure S2; arrows), and FOXL2-positive cells failed to invade the nests and surround single oocytes (Figure 2B). Abnormal germ-cell nest breakdown can lead to the formation of follicles that contain more than one oocyte, also known as polyovular follicles [35]. At postnatal day 9 in FOXL2+ ovaries, growing follicles that contained two or more oocytes were observed (Figure 2B; arrows). Incidence of polyovular follicles (Figure 2C) was significantly higher in FOXL2+ ovaries (11.33 ± 0.87% follicles) when compared to control ovaries (4.34 ± 0.37% follicles, n = 4/genotype, Student t-test $p < 0.001$).

As follicles form, each individual follicle becomes enclosed in a basal membrane. Immunostaining for FOXL2, GCNA1 (germ cell marker also known as TRA98 [36]), and laminin, a component of the basal membrane in 3-weeks old FOXL2+ ovaries revealed the presence of polyovular primordial, primary and secondary follicles (Figure 2D). In ovaries from mature FOXL2+ mice, large secondary and pre-ovulatory polyovular follicles remained present at 8 weeks and 6 months of age (Figure 2E).

FOXL2+ females develop defects in ovulation and estrous cycle

While control and FOXL2+ ovaries were grossly indistinguishable at P9 (Figure 2A), ovaries of sexually mature 8 weeks old FOXL2+ females were smaller than those of controls (Figure 3A). All stages of folliculogenesis from primordial to pre-ovulatory follicles were observed in FOXL2+ ovaries; however, no corpora lutea were present (Figure 3A; asterisks). Corpora lutea are formed by luteal cells following ovulation, and lack of corpora lutea indicates absence of ovulation [35]. In FOXL2+ ovaries, oocytes in peri-ovulatory follicles remained entrapped in the follicles and follicles became hemorrhagic (Figure 3A). Throughout adult life, FOXL2+ ovaries remained smaller than control ovaries and no corpora lutea were ever observed (Figure 3B), suggesting a complete lack of ovulation in FOXL2+ females.

To determine whether FOXL2+ mice had defects in their estrous cycle, 7-week-old females were subjected to daily vaginal smears (n = 5/genotype). All stages of the estrus cycle were observed in control females (Figure 3C) with 12.4 ± 1.6 percent of the time in proestrus, 32.8 ± 2.1% in estrus, 18 ± 1.7% in metestrus, and 36.8 ± 3.8% in diestrus. On the other hand, FOXL2+ female stayed in diestrus (97.1 ± 1.9% of the time) and no proestrus or estrus stage

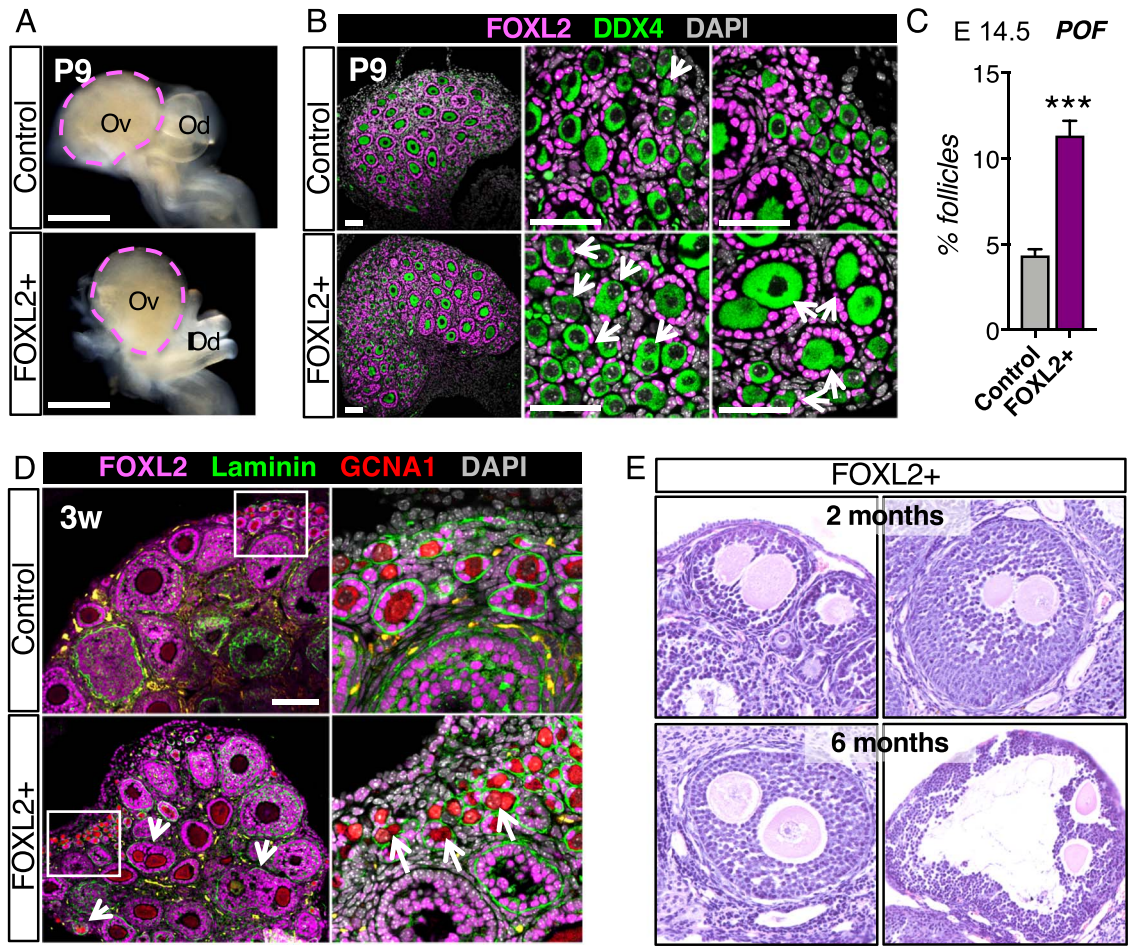

Figure 2. Overexpression of FOXL2 results in defects in germ cell nest breakdown and formation of polyovular follicles. (A) Bright field images of control and FOXL2+ ovaries at postnatal day 9 (P9). Dotted lines outline the ovaries. Ov: ovary; Od: oviduct. Scale bar: 500 µm. (B) Immunofluorescence for FOXL2 (magenta), germ cell marker DDX4, and nuclear counterstain DAPI (grey) in control and FOXL2+ ovaries at P9. Arrows indicate polyovular follicles and oocytes in nests. Scale bars: 50 µm; n = 4/genotype. (C) Quantification of polyovular follicles in control and FOXL2+ ovaries at P9. Bar graphs represent mean ± SEM (n = 4 ovaries/genotype); Student t-test ***P < 0.001. (D) Immunofluorescence for FOXL2 (magenta), Laminin (green), germ cell marker GCNA1 (red), and nuclear counterstain DAPI (grey) in 3-week old control and FOXL2+ ovaries. Arrows point to polyovular follicles. Right panels are higher magnification images of the outlined area. Scale bar: 100 µm; n = 4/genotype. Yellow staining represents autofluorescent blood cells. (E) H&E stained sections of FOXL2+ ovaries containing polyovular follicles, at 2 months and 6 months of age.

was observed (Figure 3C). Serum level of FSH were significantly higher in FOXL2+ females (58.82 ± 12.59 ng/mL, n = 6) compared to control females (16.64 ± 2.07, n = 6), while LH levels were not significantly different (Figure 3D).

Sexually mature FOXL2+ females present defects in steroidogenesis

Ovarian steroidogenesis plays a key role in the normal function of the ovary. We examined the expression of steroidogenic enzymes and serum levels of progesterone and estradiol in 8-week-old mice (Figure 4). In control ovaries (Figure 4A and Supplementary Figure S3A), the steroidogenic enzyme HSD3B was detected robustly in theca cells, interstitial cells and luteal cells in corpora lutea (asterisk) and weakly in granulosa cells as expected [37]. In contrast, in FOXL2+ ovaries, while HSD3B was normally detected in granulosa cells, only a few theca and interstitial cells were positive for HSD3B (Figure 4A arrows). Similarly, androgen producing enzyme CYP17A1 was clearly detected in the theca interna of control ovaries, but only few CYP17A1-positive cells were detected FOXL2+ ovaries despite of the presence of Smooth muscle actin (SMA)-positive interstitial cells (Figure 4B). Examination of mRNA expression by qPCR further confirmed the significant downregulation of the steroidogenic enzymes *Cyp11a1* and *Star* in FOXL2+ ovaries (Figure 4C). Serum level of progesterone in adult FOXL2+ females was significantly lower than that in the control females in diestrus (Figure 4D), likely due to the complete lack of corpora lutea (Figure 3). Despite robust expression of *Cyp19a1* in FOXL2+ ovaries (Supplementary Figure S3B), serum levels for 17β-estradiol were similar in both diestrus control and FOXL2+ females, barely above the detectable range of the test (Figure 4D).

The structural integrity of the follicles is compromised in FOXL2+ ovaries

In addition to defects in steroidogenesis, immunostaining for interstitial cell marker a SMA revealed some disorganization in the ovarian interstitium of FOXL2+ ovaries compared to control ovaries (Figure 4B). Further histological analyses of the follicles in adult FOXL2+ mice showed defects in organization at the junction

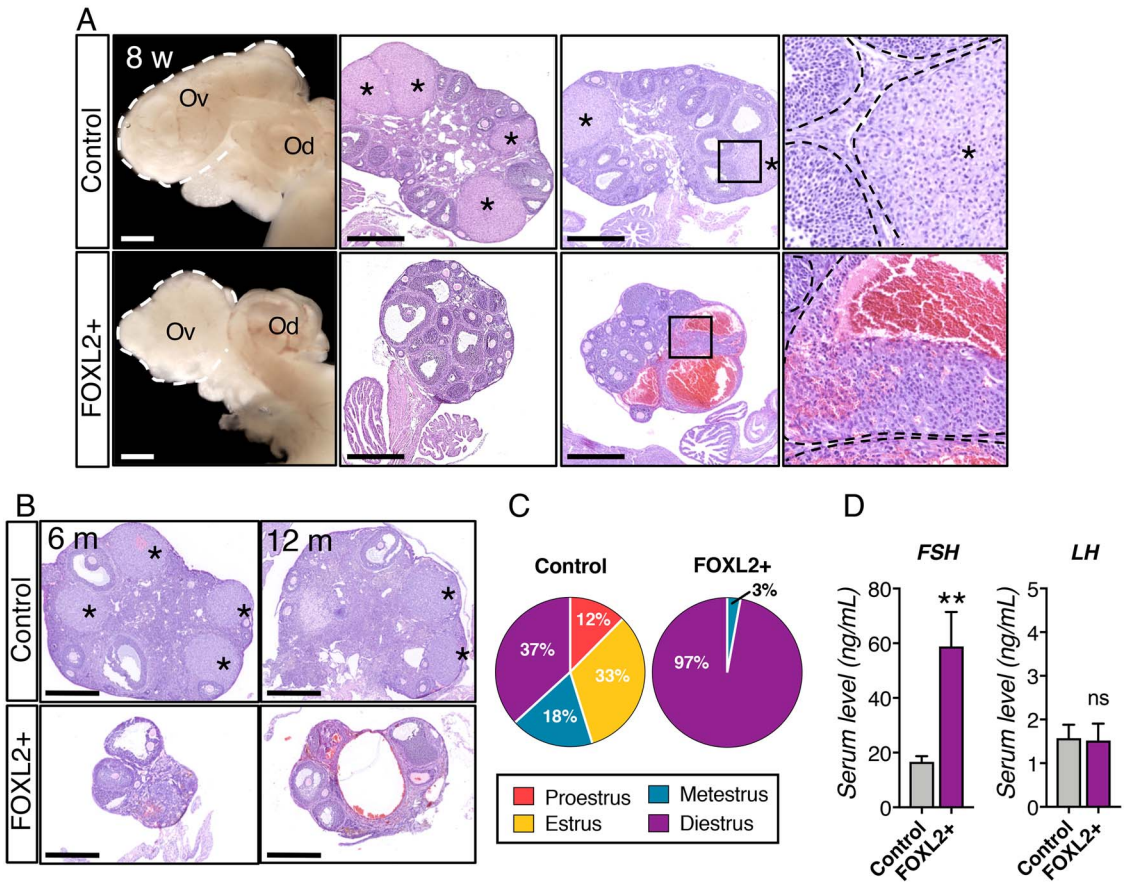

Figure 3. Absence of corpora lutea and regular estrous cycle in FOXL2+ females. (A) Bright field images and H&E stained sections of control and FOXL2+ ovaries at 8 weeks of age. White dotted lines outline the ovaries. Black dotted lines outline follicles and corpora lutea. Ov: ovary; Od: oviduct; ∗: corpus luteum; Scale bar: 500 μm; n = 4/genotype. (B) H&E stained sections of control and FOXL2+ ovaries at 6 and 12 months old. ∗: corpus luteum; Scale bar: 500 μm; n = 4/genotype. (C) Pie charts represent the mean percentage of days the mice spent in each stage of the estrous cycle (n = 5 mice/genotype). (D) Serum levels for FSH and LH in control and FOXL2+ mice at 8 weeks of age. The results were analyzed with Mann–Whitney test; mean ± SEM (n = 6/genotype); $^{**}P < 0.01$, ns: non-significant.

between granulosa and theca cells (Figure 5A). In control ovaries, antral follicles were surrounded by a well-defined theca interna with a clear separation between cuboidal-shaped granulosa cells and flatten-shaped theca cells (Figure 5A; black rectangle). In contrast in FOXL2+ antral follicles, the theca interna layer was either thin (Figure 5A; red rectangle, arrowheads), or the boundary between granulosa cells and theca cells was not well defined, resulting in an intermingling of granulosa cells and theca cells in place of the theca interna (Figure 5A; blue rectangle, arrows). Immunofluorescence for interstitial cell markers NR2F2 (also called COUP-TFII) and HSD3B in 3-week-old ovaries showed that this disorganization of the somatic compartments was already apparent in FOXL2+ ovaries before sexual maturity (Figure 5B and Supplementary Figure S4A). In control 3-week-old ovaries, both granulosa and interstitial compartments were well organized: granulosa cells were located inside of follicles and the follicles were fully surrounded by the interstitium, mostly composed of flatten NR2F2+ cells (Figure 5B and S4A). Subpopulations of the interstitium corresponding to theca cells and interstitial gland cells [37] were strongly positive for HSD3B in addition to NR2F2+ (Figure 5B). In FOXL2+ ovaries, follicles were not fully surrounded by NR2F2+ interstitial cells, resulting in incomplete delineation of the follicles (Fig. 5B, arrowheads). In controls, growing follicles occupied most of the ovarian body and the interstitium compartment was limited. This was in contrast to the expanded interstitial space in FOXL2+ ovaries. Furthermore, the composition of the interstitium was different between the control and FOXL2+ ovaries: in addition to flatten NR2F2+ cells, the FOXL2+ ovarian interstitium contained large NR2F2-negative cells with weak HSD3B expression that resembled granulosa cells (Figure 5B; arrows). Immunofluorescence for laminin (Figure 5C and Supplementary Figure S4A) showed that follicles of control ovaries were fully surrounded by laminin. However, laminin deposition around follicles of FOXL2+ ovaries was disorganized and discontinuous, leading to a mixture of granulosa cells and interstitial cells. (Fig. 5C, arrowheads). To assess whether these abnormal follicles corresponded to dying follicles, cell death TUNEL assay was performed along with immuno-labeling for Laminin and FOXL2 (Supplementary Figure S4B). It demonstrated that these abnormal follicles with irregular basal membrane did not correspond to dying atretic follicles.

Constitutive expression of FOXL2 in ovarian somatic cells impairs theca cell differentiation

Theca cells, the source of androgens, are recruited by developing follicles in the neonatal ovary [2–4]. To determine whether the defects in steroidogenesis and follicle organization in adult FOXL2+ ovary were caused by compromised theca cell recruitment and

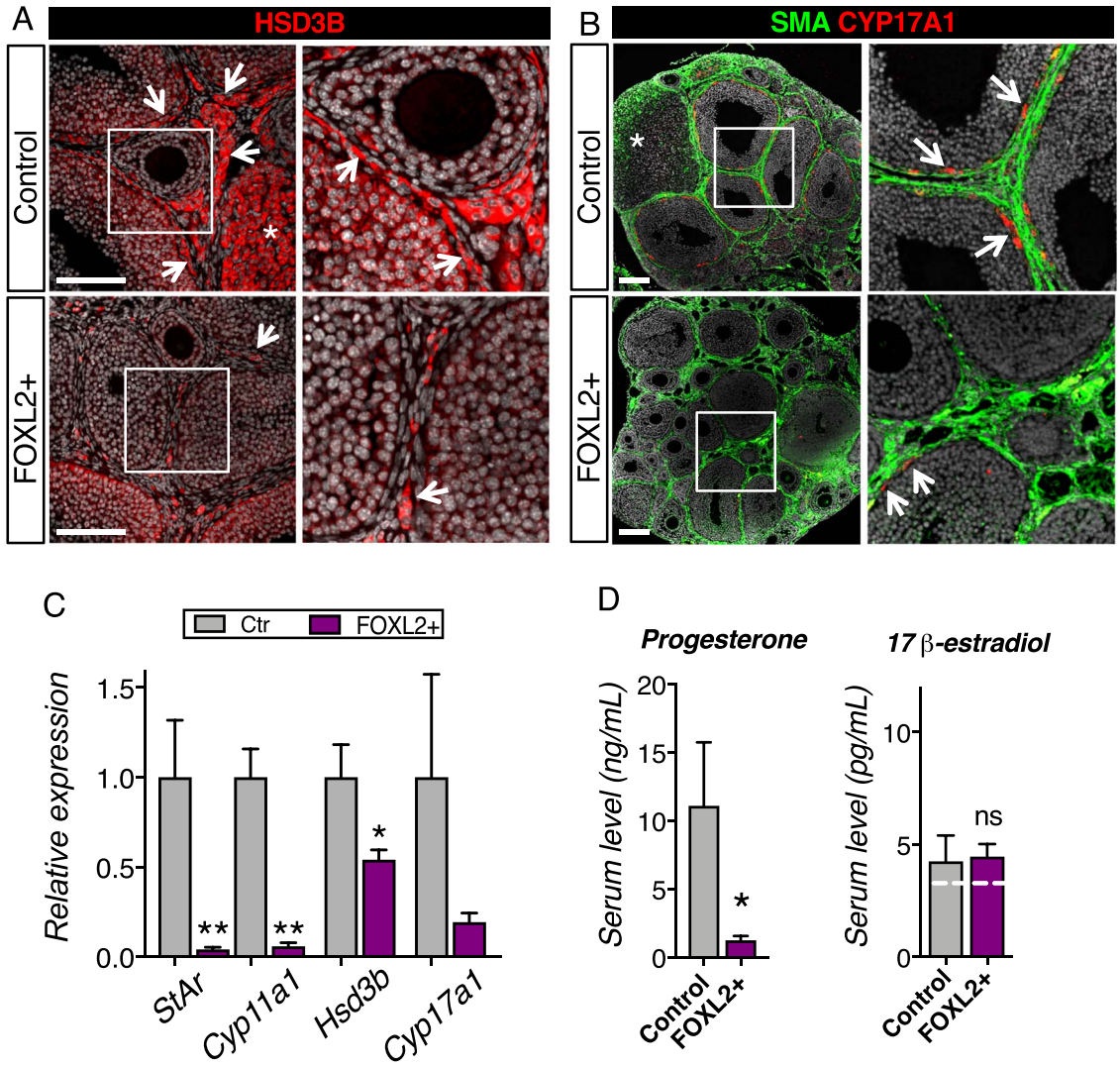

Figure 4. Overexpression of FOXL2 results in defects in steroidogenesis. (A) Immunofluorescence for the steroidogenic enzyme HSD3B in control and FOXL2+ ovaries at 8 weeks of age. Right panels are higher magnification of outlined areas. Arrows point to HSD3B+ theca/interstitial cells. ∗: HSD3B+ corpus luteum. Scale bar: 100 µm. (B) Immunofluorescence for the steroidogenic enzyme CYP17A1 and alpha smooth muscle actin (SMA) in 8-week-old control and FOXL2+ ovaries. Right panels are higher magnification of outlined areas. Arrows point to CYP17A1+ theca cells in the theca interna. ∗: corpus luteum. Scale bar: 100 µm; n = 4/genotype. (C) qPCR analysis of steroidogenic enzymes *Hsd3b, Cyp17a1, Cyp11a1* and *Star* expression in control and FOXL2+ ovaries at 8 weeks of age. The results were analyzed with a Mann–Whitney test; mean ± SEM (n = 4–6/genotype); $**P < 0.01$; $*P < 0.05$. (D) Serum levels for progesterone and 17β-estradiol in control and FOXL2+ mice at 8 weeks of age. The results were analyzed with Mann–Whitney test; mean ± SEM (n = 6/genotype). The white dotted line represents the detectable range limits for 17β-estradiol immunodetection.

differentiation in neonatal life, we examined parameters of theca cell differentiation in neonatal ovary at P9 by either immunofluorescence or qPCR (Figure 6 and Supplementary Figure S5). In P9 control ovaries, the interstitial cells surrounding follicles expressed the steroidogenic enzyme HSD3B (Figure 6A, arrows) and each follicle became clearly demarcated by the presence of SMA (Figure 6B). In addition, CYP17A1+ theca cells started to be detected at the vicinity of the follicles (Figure 6B, arrows). On the other hand, in P9 FOXL2+ ovaries, HSD3B expression was very weak in the interstitium (Figure 6A), SMA did not clearly outline the follicles and no CYP17A1+ theca cells were detected. Analyses of mRNA expression further confirmed significant downregulation of *Hsd3b*, *Acta2* (encoding for SMA) and more than 90% reduced expression of the theca cell-specific gene *Cyp17a1* (Figure 6C and Supplementary Figure S5A), Expression of two other steroidogenic genes that are theca cell specific at this stage, *Cyp11a1* and *StAR*, was also significantly reduced in P9 FOXL2+ ovaries (Figure 6C).

Theca cell recruitment relies on signals from the granulosa cells [2, 3]. To determine whether the impaired theca cell recruitment could be indirectly caused by defects in granulosa cell differentiation, we examined the expression of markers for granulosa cell differentiation and signaling for theca cell recruitment. As granulosa cells differentiate postnatally, they start expressing Anti-Mullerian Hormone (AMH) at the primary follicle stage [38]. As expected in P9 control ovaries, AMH was detected in granulosa cells of primary and secondary follicles (Figure 6A). However, in P9 FOXL2+ ovaries, follicles contained AMH-negative granulosa cells (Figure 6A, asterisks), suggesting a delay or a defect in granulosa cell differentiation. This failure to properly activate expression of AMH was further confirmed by qPCR, with more than 50% reduction in *Amh* mRNA

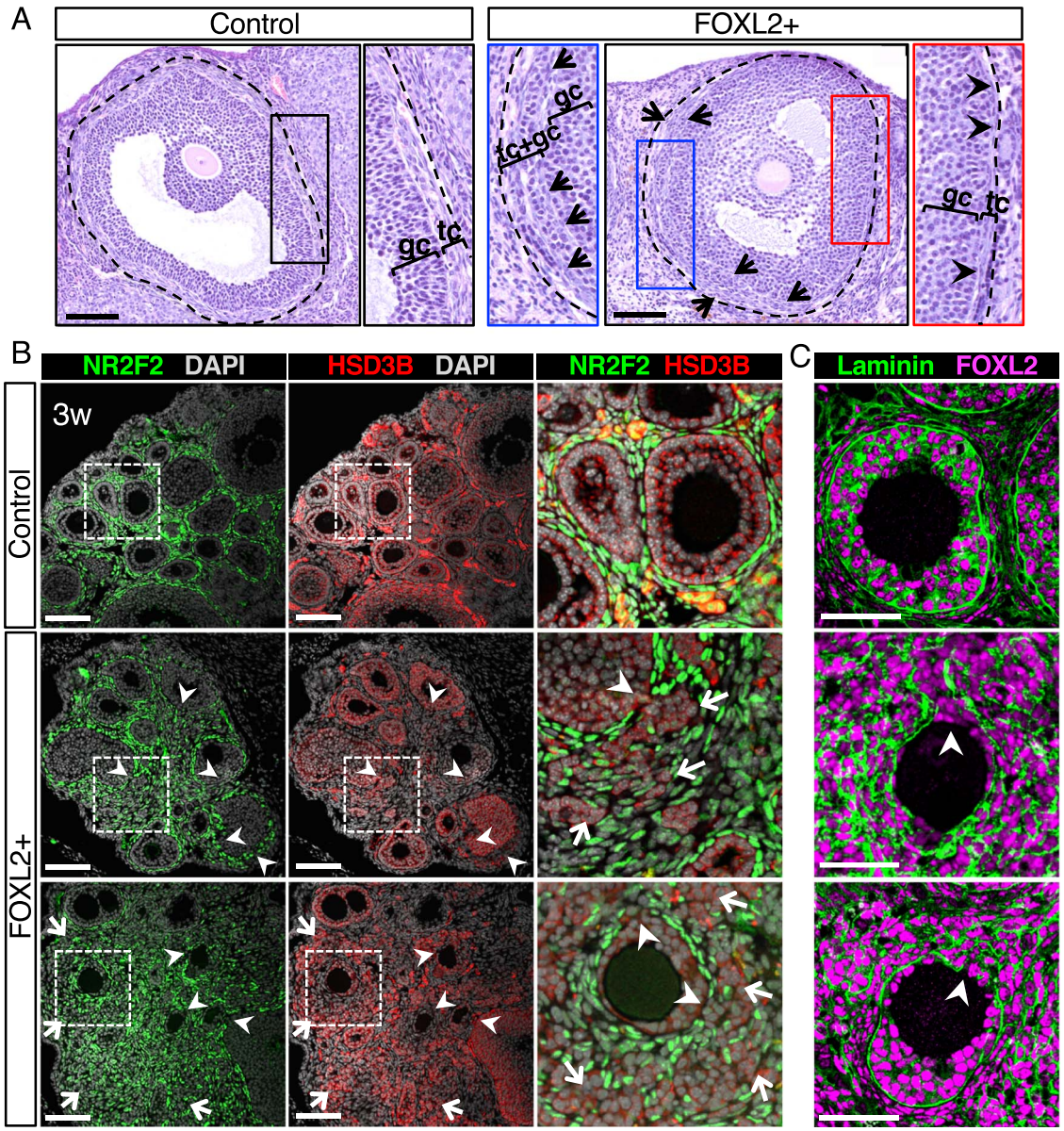

Figure 5. Structural integrity of follicles is compromised in FOXL2+ ovaries. (A) H&E stained antral follicles in adult control and FOXL2+ ovaries. The dotted lines outline the follicles that include the theca interna. Black, blue and red panels represent higher magnification of the respective outlined areas. Arrows indicate flatten theca cells mixed with granulosa cells. Arrowheads point to the theca interna. gc: granulosa cells; tc: theca cells. Scale bar: 100 μm; n = 4/genotype. (B) Immunofluorescence for the interstitial cell marker NR2F2 (green), the steroidogenic enzyme HSD3B, and nuclear counterstain DAPI (grey) in control and FOXL2+ ovaries at 3 weeks of age. The three color-merged panels represent a higher magnification of the outlined square areas. Arrowheads indicate gaps at the junction between granulosa and theca layers. Arrows point to a mixture of granulosa and interstitial cells. Scale bar: 100 μm; n = 4/genotype. (C) Immunofluorescence for FOXL2 and laminin in control and FOXL2+ ovaries at 3 weeks of age. Arrowheads indicate incomplete surrounding of follicles by Laminin in FOXL2+ ovaries. Scale bar: 50 μm; n = 4/genotype.

in FOXL2+ ovaries compared to control ovaries (Figure 6D). In addition to AMH, mRNA expression of granulosa cell-derived factors Desert hedgehog (*Dhh*) and Indian hedgehog (*Ihh*), which are responsible for recruitment of theca cells [2, 3, 39], was significantly downregulated (Figure 6D). To further assess whether FOXL2+ ovaries develop defects in granulosa cell differentiation, we examined the expression of the granulosa cell marker WT1 in 3-weeks old control and FOXL2+ ovaries (Supplementary Figure S5B). As expected [40], WT1 was strongly expressed primordial, primary and secondary follicles of control ovaries. However, in FOXL2+ ovaries, granulosa cells of some primary and secondary follicles failed to express WT1. Overall, these results indicate that postnatal differentiation of granulosa cells and theca cells was impaired in FOXL2+ ovaries.

Discussion

This study reveals that fine-tuned expression of FOXL2 is required for proper ovarian development and function. While FOXL2 is normally expressed in granulosa cells and sub-populations of interstitial

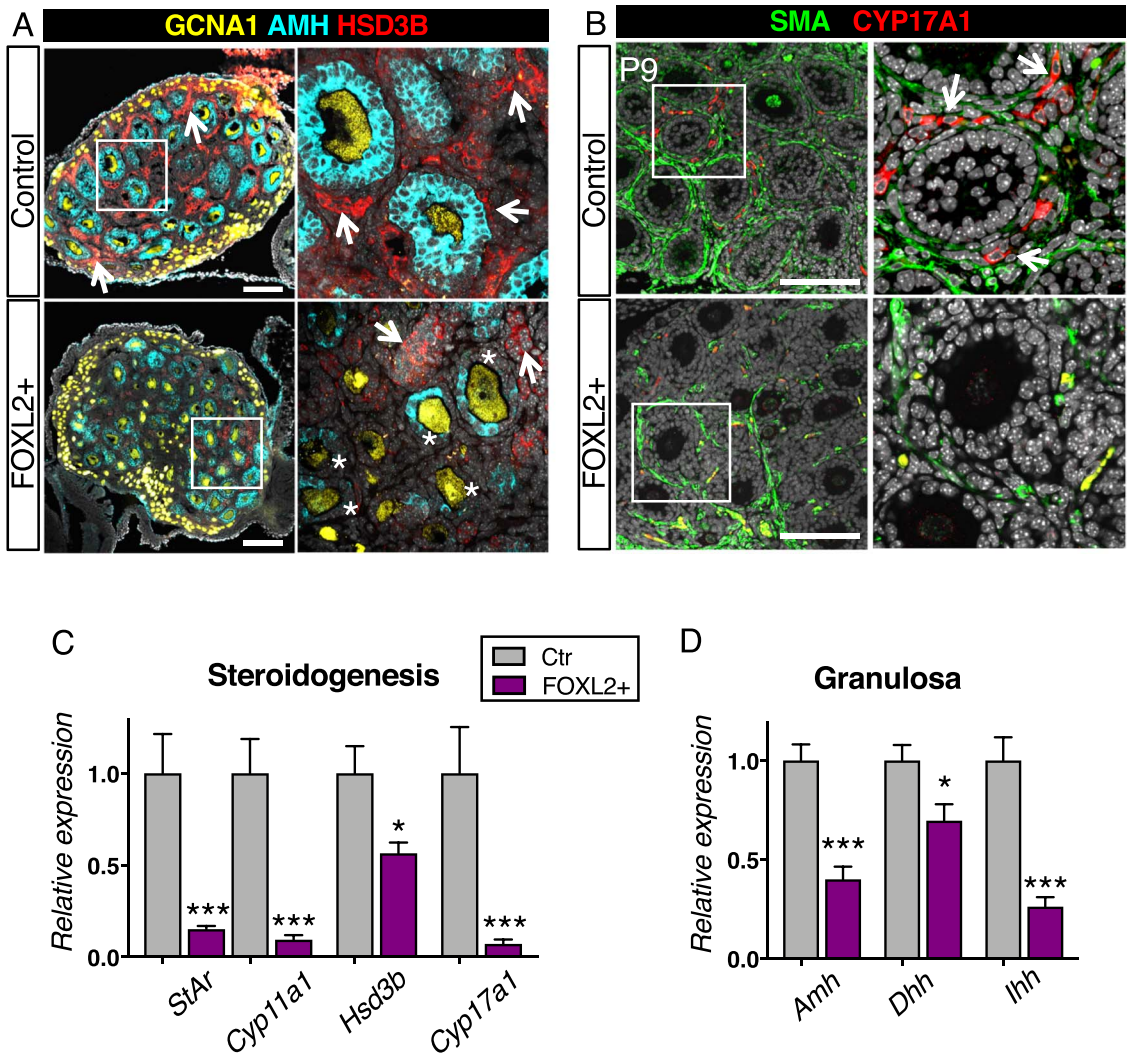

Figure 6. Overexpression of FOXL2 impairs theca cell differentiation. (A) Immunofluorescence for the steroidogenic enzyme HSD3B (red), granulosa cell marker AMH (cyan) and germ cell marker GCNA1 (yellow) in control and FOXL2+ ovaries at postnatal day 9 (P9). Right panels are higher magnification of outlined areas. Arrows indicate HSD3B+ theca/interstitial cells. ∗: AMH-negative granulosa cells. Scale bar: 100 µm; n = 4/genotype. (B) Immunofluorescence for the steroidogenic enzyme CYP17A1 (red) and SMA (green) in control and FOXL2+ ovaries at P9. Right panels are higher magnification of outlined areas. Arrows indicate CYP17A1+ theca cells. Scale bar: 100 µm; n = 4/genotype. The yellow staining represents autofluorescent blood cells. (C-D) qPCR analysis of expression of steroidogenic enzymes *Hsd3b*, *Cyp17a1*, *Cyp11a1* and *Star* (C) and granulosa cell genes *Amh*, *Dhh* and *Ihh* (D) in control and FOXL2+ ovaries at P9. The data were analyzed with a Student t-test; Bar graphs represent mean ± SEM (n = 7–8/genotype); ∗∗∗$P < 0.001$; ∗$P < 0.05$.

cells, its overexpression compromises differentiation of granulosa cells and theca cells in the postnatal ovary, resulting in defects in folliculogenesis, steroidogenesis and ovulation.

FOXL2+ adult ovaries display low expression of steroidogenic enzymes. In the ovary, the production of steroidogenic hormones relies on the cross-talk between theca and granulosa cell populations. Theca cells produce androgens that would then be converted to estrogens by granulosa cells. The reduced expression of steroidogenic enzymes in FOXL2+ ovaries implies a defect in theca cell differentiation or function. Recruitment and differentiation of theca cells in the postnatal ovary is not a cell autonomous event, it requires signaling from the granulosa cells. The fact that FOXL2 over-expression is induced in both granulosa cells and interstitial cells suggests at least two possibilities that could explain defects in theca cell differentiation/function and steroidogenesis: 1) these defects could be directly caused by FOXL2 over-expression in theca cell precursors, therefore impairing their differentiation; and 2) these defects could derive from improper signals from granulosa cells, consequently affecting theca cell differentiation. The first hypothesis is based on previous studies demonstrating that FOXL2 is capable of controlling expression of steroidogenic enzymes. For instance, FOXL2 binds the human *Star* promoter in order to suppress its activity [41]. FOXL2 also directly inhibits expression of *Cyp17a1* induced by steroidogenic factor-1 NR5A1 [42]. In both cases, FOXL2 acts as a transcriptional repressor by directly interacting with NR5A1. These observations suggest that downregulation of *Star* and *Cyp17a1* in FOXL2+ ovaries may be the result of direct transcriptional repression by ectopic FOXL2 in theca cell progenitors. NR5A1 is a master regulator of steroidogenic genes, and over-expression of FOXL2 in NR5A1-positive cells may affect NR5A1 activity, leading to downregulation of multiple steroidogenic genes.

The second possibility we propose is that impaired theca cell differentiation/function could be due to defects in granulosa cells themselves. Indeed, acquisition of androgen-producing capacity by theca cell progenitors requires Hh signaling produced by granulosa cells [2, 3, 39]. Multiple aspects of FOXL2+ ovary phenotype point to a defect or delay in granulosa cell differentiation in the postnatal ovary, such as a delay in nest-breakdown/follicle formation and impaired activation of granulosa-cell specific genes at the onset of folliculogenesis. Granulosa cells recruit steroidogenic cells by producing the Hedgehog morphogens DHH and IHH [2, 3]. Previous studies hinted to a potential regulation of Hedgehog signaling by FOXL2: in the absence of *Foxl2*, expression of *Dhh* is increased in the ovary whereas overexpression of FOXL2 in the testis represses the expression of *Dhh* [26, 43]. We found that FOXL2+ postnatal ovaries have significant downregulation of multiple members of the Hedgehog pathway such as *Dhh*, *Ihh*, *Ptch1* and *Ptch2*. Among these genes, *Ihh* was the most downregulated one. *Ihh* is the most potent Hedgehog ligand for the differentiation of theca cells and proper steroidogenesis [3]. FOXL2+ ovaries share common features with *Dhh/Ihh* double knockout ovaries, including no or very little *Hsd3b* expression, reduced steroidogenesis, abnormal interstitium, and a lack of corpora lutea and ovulation. Expression of *Dhh* and *Ihh* in granulosa cells relies on production of GDF9 by the oocytes, and absence of *Gdf9* impairs theca cell differentiation [2]. However, expression of *Gdf9* was not changed in FOXL2+ ovaries, suggesting that the defects in theca cell differentiation does not arise from the absence of signal from oocytes. Rather, the defects are initiated either by the miscommunication from granulosa cells or/and by a direct transcriptional repression of steroidogenic enzymes by FOXL2 in theca cell precursors.

The involvement of granulosa cells in the phenotypes of FOXL2+ ovaries is further supported by the common phenotypic features between FOXL2+ and *Foxl2* KO ovaries [17]. Being the main target of FOXL2 in the ovary, granulosa cells are considered the primary source of defects observed in *Foxl2* KO ovaries. Similar to FOXL2+ ovaries, *Foxl2* KO ovaries developed defects in nest-breakdown, with persistence of clusters of oocytes beyond the first week of life. In both *Foxl2* KO and FOXL2+ models, laminin distribution was abnormal, resulting in irregular thickness and fragmented deposition around follicles [17]. These two phenotypes are likely the outcome of impaired differentiation of granulosa cells at early stages of folliculogenesis. Differentiation of theca cells and consequent steroidogenesis were also impaired in *Foxl2* KO ovaries, where no *Cyp11a1*-positive cells could be detected [17]. Therefore, fine-tuned expression of FOXL2 is required for proper differentiation of granulosa and theca cells at the onset of folliculogenesis, and too much FOXL2 expression or absence of FOXL2 consequently causes primary ovarian insufficiency. There is however a major difference between FOXL2+ and *Foxl2* KO ovaries further in folliculogenesis: *Foxl2* KO follicles failed to develop further than early secondary stage [17], likely due to the progressive transdifferentiation of granulosa cells into Sertoli-like cells [21]. However, this transdifferentiation phenotype was not found in the FOXL2+ ovary.

Female fertility relies on not only the ovary, but also hormonal communications between the hypothalamus, pituitary, and ovary. While early folliculogenesis relies mostly on the ovarian microenvironment, antral follicular growth, steroidogenesis and ovulation depend on both ovarian microenvironment and the hypothalamus and pituitary through the timely secretion of FSH and LH. NR5A1-positive cells are also found in the hypothalamus and the pituitary [27]. It is therefore possible that FOXL2 constitutive expression in these two organs could indirectly affect the ovarian phenotype in FOXL2+ mice. The presence of antral and peri-ovulatory follicles in FOXL2+ ovaries suggests that FSH signaling is present. Serum measurements revealed that FOXL2+ females actually produced significantly higher levels of FSH than control females. This observation suggests an improper function of the pituitary. In the pituitary, transcription of *Fshb* is regulated by FOXL2 and loss of *Foxl2* results in decreased FSH production [44]. It is therefore possible that overexpression of FOXL2 in the pituitary is directly responsible for this increase in FSH production. Ovulation, which is completely lacking in FOXL2+ mice, relies on the synergistic action of FSH and LH. However, increase in FSH secretion is usually associated with an increase in follicle development, ovulation and estrogen production [45]. With the exception of the common presence of hemorrhagic follicles, such characteristics are not observed in FOXL2+ females, suggesting that the ovary itself may not be able to properly respond to the pituitary signal. On the other hand, while serum LH levels were not different between diestrus control and FOXL2+ females, it is possible that pulsatile secretion of LH is impaired in FOXL2+ females and contributes to the lack of ovulation. A way to determine whether the absence of ovulation is due to the hypothalamo-pituitary axis rather than the ovary would be to bypass this axis by injecting gonadotropins to artificially superovulate the mouse. However, the FOXL2+ mice were very sensitive to stress and presented high rates of lethality, likely due to defects in adrenal formation, another organ targeted by *Sf1*-Cre. This unfortunately prevented us from performing superovulation experiments and fertility studies.

Finally, none of the females with over-expression of FOXL2 developed granulosa cell tumors. A specific mutation in *FOXL2* gene is found in the majority of adult granulosa cell tumors in women [9] and homozygosity for this mutation is associated with recurrence of these tumors [46]. However, this mutation does not alter *FOXL2* expression itself [47], but it rather appears to impair anti-proliferative and pro-apoptotic capacities of FOXL2 [10, 11]. On the other hand, juvenile granulosa cell tumors, which do not harbor this mutation, present a low expression of FOXL2 that is correlated with the aggressiveness of the tumor [48]. Therefore, granulosa cell tumors appear to correlate with either reduced function or reduced expression of FOXL2 rather than an over-expression of FOXL2.

In summary, we show that aberrant expression of FOXL2 in NR5A1-positive somatic cells impacts several key developmental and functional aspects of the ovary. Female mice overexpressing FOXL2 presented defects in granulosa cell and theca cell differentiation and in the hypothalamic–pituitary–gonadal axis communication. As a result, FOXL2+ ovaries had impaired oocyte nest breakdown, follicle compartmentalization and steroidogenesis, ultimately leading to complete anovulation. While in normal conditions FOXL2 is expressed in granulosa cells, the interstitial compartment and the pituitary, fine-tuned expression of FOXL2 in these cell populations is required for proper ovarian physiology and fertility.

Supplementary data

Supplementary data are available at *BIOLRE* online.

Conflict of interest

The authors declare no competing financial or non-financial interests.

Author contributions

HY and BN conceived the study; HY supervised the project; BN and KR performed the experiments and analyzed the data; BN and HY wrote the manuscript. All authors read and approved the final manuscript.

Acknowledgements

We thank the late Dr. Keith Parker (UT Southwestern Medical Center) for the *Sf1*-Cre mice and Ken Morohashi (Kyushu University, Japan) for the NR5A1 antibody. We are grateful to the NIEHS Comparative Medicine Branch for mouse colony maintenance, and NIEHS Cellular and Molecular Pathology Branch for histological imaging. We also thank the University of Virginia Center for Research in Reproduction Ligand Assay and Analysis Core, which is supported by the Eunice Kennedy Shriver NICHD/NIH Grant R24HD102061.

References

1. Dong J, Albertini DF, Nishimori K, Kumar TR, Lu N, Matzuk MM. Growth differentiation factor-9 is required during early ovarian folliculogenesis. *Nature* 1996; **383**:531–535.
2. Liu C, Peng J, Matzuk MM, Yao HH. Lineage specification of ovarian theca cells requires multicellular interactions via oocyte and granulosa cells. *Nat Commun* 2015; **6**:6934.
3. Liu C, Rodriguez KF, Brown PR, Yao HH. Reproductive, physiological, and molecular outcomes in female mice deficient in Dhh and Ihh. *Endocrinology* 2018; **159**:2563–2575.
4. Richards JS, Ren YA, Candelaria N, Adams JE, Rajkovic A. Ovarian follicular theca cell recruitment, differentiation, and impact on fertility: 2017 update. *Endocr Rev* 2018; **39**:1–20.
5. Crisponi L, Deiana M, Loi A, Chiappe F, Uda M, Amati P, Bisceglia L, Zelante L, Nagaraja R, Porcu S, Ristaldi MS, Marzella R et al. The putative forkhead transcription factor FOXL2 is mutated in blepharophimosis/ptosis/epicanthus inversus syndrome. *Nature Genetics* 2001; **27**: 159–166.
6. Dipietromaria A, Benayoun BA, Todeschini AL, Rivals I, Bazin C, Veitia RA. Towards a functional classification of pathogenic FOXL2 mutations using transactivation reporter systems. *Hum Mol Genet* 2009; **18**:3324–3333.
7. Harris SE, Chand AL, Winship IM, Gersak K, Aittomaki K, Shelling AN. Identification of novel mutations in FOXL2 associated with premature ovarian failure. *Mol Hum Reprod* 2002; **8**:729–733.
8. Laissue P, Lakhal B, Benayoun BA, Dipietromaria A, Braham R, Elghezal H, Philibert P, Saad A, Sultan C, Fellous M, Veitia RA. Functional evidence implicating FOXL2 in non-syndromic premature ovarian failure and in the regulation of the transcription factor OSR2. *J Med Genet* 2009; **46**:455–457.
9. Shah SP, Kobel M, Senz J, Morin RD, Clarke BA, Wiegand KC, Leung G, Zayed A, Mehl E, Kalloger SE, Sun M, Giuliany R et al. Mutation of FOXL2 in granulosa-cell tumors of the ovary. *N Engl J Med* 2009; **360**:2719–2729.
10. Benayoun BA, Georges AB, L'Hote D, Andersson N, Dipietromaria A, Todeschini AL, Caburet S, Bazin C, Anttonen M, Veitia RA. Transcription factor FOXL2 protects granulosa cells from stress and delays cell cycle: Role of its regulation by the SIRT1 deacetylase. *Hum Mol Genet* 2011; **20**:1673–1686.
11. Kim JH, Yoon S, Park M, Park HO, Ko JJ, Lee K, Bae J. Differential apoptotic activities of wild-type FOXL2 and the adult-type granulosa cell tumor-associated mutant FOXL2 (C134W). *Oncogene* 2011; **30**:1653–1663.
12. Fleming NI, Knower KC, Lazarus KA, Fuller PJ, Simpson ER, Clyne CD. Aromatase is a direct target of FOXL2: C134W in granulosa cell tumors via a single highly conserved binding site in the ovarian specific promoter. *PLoS One* 2010; **5**:e14389.
13. Bertho S, Pasquier J, Pan Q, Le Trionnaire G, Bobe J, Postlethwait JH, Pailhoux E, Schartl M, Herpin A, Guiguen Y. Foxl2 and its relatives are evolutionary conserved players in gonadal sex differentiation. *Sex Dev* 2016; **10**:111–129.
14. Loffler KA, Zarkower D, Koopman P. Etiology of ovarian failure in blepharophimosis ptosis epicanthus inversus syndrome: FOXL2 is a conserved, early-acting gene in vertebrate ovarian development. *Endocrinology* 2003; **144**:3237–3243.
15. Mork L, Maatouk DM, McMahon JA, Guo JJ, Zhang P, McMahon AP, Capel B. Temporal differences in Granulosa cell specification in the ovary reflect distinct follicle fates in mice. *Biology of Reproduction* 2012; **86**.
16. Schmidt D, Ovitt CE, Anlag K, Fehsenfeld S, Gredsted L, Treier AC, Treier M. The murine winged-helix transcription factor Foxl2 is required for granulosa cell differentiation and ovary maintenance. *Development* 2004; **131**:933–942.
17. Uda M, Ottolenghi C, Deiana M, Kimber W, Forabosco A, Cao A, Schlessinger D, Pilia G. Foxl2 disruption causes mouse ovarian failure by pervasive blockage of follicle development. *Human Molecular Genetics* 2004; **13**:1171–1181.
18. Boulanger L, Pannetier M, Gall L, Allais-Bonnet A, Elzaiat M, Le Bourhis D, Daniel N, Richard C, Cotinot C, Ghyselinck NB, Pailhoux E. FOXL2 is a female sex-determining gene in the goat. *Curr Biol* 2014; **24**: 404–408.
19. Li M, Yang H, Zhao J, Fang L, Shi H, Li M, Sun Y, Zhang X, Jiang D, Zhou L, Wang D. Efficient and heritable gene targeting in tilapia by CRISPR/Cas9. *Genetics* 2014; **197**:591–599.
20. Major AT, Ayers K, Chue J, Roeszler K, Smith C. FOXL2 antagonises the male developmental pathway in embryonic chicken gonads. *J Endocrinol* 2019.
21. Ottolenghi C, Omari S, Garcia-Ortiz JE, Uda M, Crisponi L, Forabosco A, Pilia G, Schlessinger D. Foxl2 is required for commitment to ovary differentiation. *Human Molecular Genetics* 2005; **14**:2053–2062.
22. Uhlenhaut NH, Jakob S, Anlag K, Eisenberger T, Sekido R, Kress J, Treier A-C, Klugmann C, Klasen C, Holter NI, Riethmacher D, Schuetz G et al. Somatic sex reprogramming of adult ovaries to testes by FOXL2 ablation. *Cell* 2009; **139**:1130–1142.
23. Ottolenghi C, Pelosi E, Tran J, Colombino M, Douglass E, Nedorezov T, Cao A, Forabosco A, Schlessinger D. Loss of Wnt4 and Foxl2 leads to female-to-male sex reversal extending to germ cells. *Human Molecular Genetics* 2007; **16**:2795–2804.
24. Auguste A, Chassot AA, Gregoire EP, Renault L, Pannetier M, Treier M, Pailhoux E, Chaboissier MC. Loss of R-spondin1 and Foxl2 amplifies female-to-male sex reversal in XX mice. *Sex Dev* 2011; **5**:304–317.
25. Nicol B, Grimm SA, Chalmel F, Lecluze E, Pannetier M, Pailhoux E. Dupin-De-Beyssat E, Guiguen Y, Capel B, Yao HH. RUNX1 maintains the identity of the fetal ovary through an interplay with FOXL2. *Nat Commun* 2019; **10**:5116.
26. Nicol B, Grimm SA, Gruzdev A, Scott GJ, Ray MK, Yao HH. Genome-wide identification of FOXL2 binding and characterization of FOXL2 feminizing action in the fetal gonads. *Hum Mol Genet* 2018; **27**:4273–4287.
27. Bingham NC, Verma-Kurvari S, Parada LF, Parker KL. Development of a steroidogenic factor 1/Cre transgenic mouse line. *Genesis* 2006; **44**:419–424.
28. Nicol B, Yao HH. Gonadal identity in the absence of pro-testis factor SOX9 and pro-ovary factor Beta-catenin in mice. *Biol Reprod* 2015; **93**:35.
29. Maatouk DM, DiNapoli L, Alvers A, Parker KL, Taketo MM, Capel B. Stabilization of beta-catenin in XY gonads causes male-to-female sex-reversal. *Human Molecular Genetics* 2008; **17**:2949–2955.
30. Lavery R, Chassot AA, Pauper E, Gregoire EP, Klopfenstein M, de Rooij DG, Mark M, Schedl A, Ghyselinck NB, Chaboissier MC. Testicular differentiation occurs in absence of R-spondin1 and Sox9 in mouse sex reversals. *PLoS Genet* 2012; **8**:e1003170.
31. Cora MC, Kooistra L, Travlos G. Vaginal cytology of the laboratory rat and mouse: Review and criteria for the staging of the Estrous cycle using stained vaginal smears. *Toxicol Pathol* 2015; **43**:776–793.

32. Maatouk DM, Mork L, Hinson A, Kobayashi A, McMahon AP, Capel B. Germ cells are not required to establish the female pathway in mouse fetal gonads. *PLoS One* 2012; **7**:e47238.
33. Zheng W, Zhang H, Liu K. The two classes of primordial follicles in the mouse ovary: Their development, physiological functions and implications for future research. *Mol Hum Reprod* 2014; **20**:286–292.
34. Tingen C, Kim A, Woodruff TK. The primordial pool of follicles and nest breakdown in mammalian ovaries. *Mol Hum Reprod* 2009; **15**:795–803.
35. Richards JS, Pangas SA. The ovary: Basic biology and clinical implications. *J Clin Invest* 2010; **120**:963–972.
36. Carmell MA, Dokshin GA, Skaletsky H, Hu YC, van Wolfswinkel JC, Igarashi KJ, Bellott DW, Nefedov M, Reddien PW, Enders GC, Uversky VN, Mello CC et al. A widely employed germ cell marker is an ancient disordered protein with reproductive functions in diverse eukaryotes. *Elife* 2016; **5**.
37. Miyabayashi K, Tokunaga K, Otake H, Baba T, Shima Y, Morohashi K. Heterogeneity of ovarian theca and interstitial gland cells in mice. *PLoS One* 2015; **10**:e0128352.
38. Durlinger AL, Kramer P, Karels B, de Jong FH, Uilenbroek JT, Grootegoed JA, Themmen AP. Control of primordial follicle recruitment by anti-Mullerian hormone in the mouse ovary. *Endocrinology* 1999; **140**:5789–5796.
39. Spicer LJ, Sudo S, Aad PY, Wang LS, Chun SY, Ben-Shlomo I, Klein C, Hsueh AJ. The hedgehog-patched signaling pathway and function in the mammalian ovary: A novel role for hedgehog proteins in stimulating proliferation and steroidogenesis of theca cells. *Reproduction* 2009; **138**:329–339.
40. Hsu SY, Kubo M, Chun SY, Haluska FG, Housman DE, Hsueh AJ. Wilms' tumor protein WT1 as an ovarian transcription factor: Decreases in expression during follicle development and repression of inhibin-alpha gene promoter. *Mol Endocrinol* 1995; **9**:1356–1366.
41. Pisarska MD, Bae J, Klein C, Hsueh AJW. Forkhead L2 is expressed in the ovary and represses the promoter activity of the steroidogenic acute regulatory gene. *Endocrinology* 2004; **145**:3424–3433.
42. Park M, Shin E, Won M, Kim JH, Go H, Kim HL, Ko JJ, Lee K, Bae J. FOXL2 interacts with steroidogenic factor-1 (SF-1) and represses SF-1-induced CYP17 transcription in granulosa cells. *Mol Endocrinol* 2010; **24**:1024–1036.
43. Garcia-Ortiz JE, Pelosi E, Omari S, Nedorezov T, Piao Y, Karmazin J, Uda M, Cao A, Cole SW, Forabosco A, Schlessinger D, Ottolenghi C. Foxl2 functions in sex determination and histogenesis throughout mouse ovary development. *BMC Dev Biol* 2009; **9**:36.
44. Ongaro L, Schang G, Zhou Z, Kumar TR, Treier M, Deng CX, Boehm U, Bernard DJ. Human follicle-stimulating hormone ß subunit expression depends on FOXL2 and SMAD4. *Endocrinology* 2020; **161**.
45. McDonald R, Sadler C, Kumar TR. Gain-of-function genetic models to study FSH action. *Front Endocrinol (Lausanne)* 2019; **10**:28.
46. Kraus F, Dremaux J, Altakfi W, Goux M, Pontois L, Sevestre H, Trudel S. FOXL2 homozygous genotype and chromosome instability are associated with recurrence in adult granulosa cell tumors of the ovary. *Oncotarget* 2020; **11**:419–428.
47. Jamieson S, Butzow R, Andersson N, Alexiadis M, Unkila-Kallio L, Heikinheimo M, Fuller PJ, Anttonen M. The FOXL2 C134W mutation is characteristic of adult granulosa cell tumors of the ovary. *Mod Pathol* 2010; **23**:1477–1485.
48. Kalfa N, Philibert P, Patte C, Ecochard A, Duvillard P, Baldet P, Jaubert F, Fellous M, Sultan C. Extinction of FOXL2 expression in aggressive ovarian granulosa cell tumors in children. *Fertil Steril* 2007; **87**:896–901.